

**A Stable and Sustainable Environmental Energy Source for Continuous Thermal-to-Electric Energy Conversion Utilizing the Effect of Acceleration Forces Causing Internal Voltage Gradients**

Kuo Tso Chen

OPTROMAX Co. Taiwan, Zhudong Township, Hsinchu County 310658, Taiwan (R.O.C.)

**CORRESPONDING AUTHOR**

E-mail: [gtchen0@gmail.com](mailto:gtchen0@gmail.com).

Phone: +886-918-629-588

## **ABSTRACT**

The second law of thermodynamics is widely regarded as unbreakable, with past attempts to refute it failing under scrutiny. In 2015, the author hypothesized that gravity could impart a directional component to molecular motion, potentially converting thermal energy into electrical energy without requiring a temperature difference. This hypothesis, which was extended to plasmas and electrolytes with ions of differing masses by 2022, was experimentally confirmed later that year. Tolman reported a similar electromotive force (EMF) in electrolytes under centrifugal and gravitational fields in 1910, although no prior research connected his findings to thermodynamics. Our study revisits this overlooked phenomenon, demonstrating how ionic solutions under a gravitational or centrifugal field generate a significant potential difference due to mass-dependent ion behavior, and how this potential difference differs from that of metals. Ionic solutions produce measurable and sustained EMFs, which can drive a current when connected in a conductive loop. We theoretically and experimentally validate that the current remains continuous, as any deviation from equilibrium during electron exchange creates a driving force that re-establishes the potential difference. Thermal vibrations promote the diffusion of ions toward equilibrium, whereas the generated voltage continuously maintains a balance between these opposing forces, enabling stable and sustained energy conversion. As a concrete example, we show that using hydrogen iodide (HI) under specified conditions can theoretically produce approximately 72 W per cubic meter of electrolyte and material, highlighting its potential as a stable and emission-free energy source. These findings reinforce Tolman's results and provide a novel thermodynamic framework for energy conversion.

## 1. INTRODUCTION

In today's energy landscape, addressing global warming and finding effective energy conversion methods are critical challenges. Many energy systems rely on converting thermal energy into mechanical or electrical energy. However, according to Carnot's theorem<sup>1</sup>, once heat is transferred from a high-temperature region to a low-temperature region and loses its temperature gradient, the thermal energy can no longer be converted into usable energy.

The second law of thermodynamics<sup>2</sup> is considered an unbreakable iron law. Historically, any claims of violating this law have been proven incorrect<sup>3</sup>. However, we believe that there may still be a possibility to transcend this law. In 2015, the author of this paper realized that the gravitational force gives molecular motion directionality rather than being entirely random, suggesting that a setup involving gravity or a centrifugal force could surpass the second law of thermodynamics, which is based on random motion. By 2021, it was hypothesized that plasmas in the upper atmosphere might exhibit such properties. In April 2022, electrolytic solutions were also noted to contain charged particles of different masses, which might exhibit the same phenomenon. After the experiments were conducted, this hypothesis was confirmed in August 2022. Later, in November 2024, the author discovered that Tolman experimentally demonstrated the existence of an electromotive force (EMF) in electrolytes under centrifugal and gravitational fields as early as 1910<sup>4</sup>, which aligns precisely with the author's experimental findings.

However, it is intriguing why, for over a century, no one identified Tolman's conclusions as a means to surpass the limitations of the second law of thermodynamics.

Simply put, as Tolman concluded in 1916, the potential difference produced by metals in a gravitational field is far smaller than that of ionic solutions<sup>5</sup>. Therefore, in a gravitational field, if the top and bottom of an ionic liquid column are connected by a metal, the metal's potential

difference is negligible, and the potential difference between the top and bottom of the ionic liquid column will induce a current within the metal, allowing it to output electrical energy. After generating a current, the electrolyte deviates from equilibrium due to electron exchange, causing the current to stop. However, the 'thermal energy' driving 'thermal vibrations' will diffuse the molecules back toward equilibrium, reestablishing the potential difference and producing the next current. While Tolman attributed the generation of voltage to a form of polarization<sup>4</sup>, the author proposed a different interpretation. The author suggested that thermal vibrations disrupt the stable relative positions of positive and negative ions, thereby disturbing this polarization phenomenon. The energy from thermal vibrations drives the diffusion motion of ions, continuously pushing their distribution back to a state of equilibrium with gravitational or centrifugal forces. This process sustains the voltage difference while simultaneously enabling a continuous flow of current. Thus, thermal energy is converted to electrical energy without requiring a temperature difference, effectively transcending the second law of thermodynamics.

This phenomenon was investigated by Colley (1882), who examined its impact on electrolytes and demonstrated that acceleration could directly affect current flow in such materials<sup>6</sup>. Des Coudres (1892) extended these studies, noting the centrifugal effects on electrolytes, which provided further insight into the role of acceleration in ion movement<sup>7</sup>. These early studies laid the foundation for understanding how ions, owing to their larger mass than that of electrons, could exhibit distinctive behaviors under acceleration, particularly in electrolyte systems. Subsequent practical applications of this phenomenon have been widely studied. For example, in 2011, L. Lao, C. Ramshaw, and H. Yeung conducted research on enhancing the process of water electrolysis in a centrifugal acceleration field<sup>8</sup>.

While this phenomenon has been widely studied, there has been little research on its potential to break the thermal energy conversion limits and convert heat into electrical energy without relying on a temperature gradient. The scientific community has largely adhered to the second law of thermodynamics, rarely considering this possibility. This is precisely because no one has approached this issue from a thermodynamic perspective for over a century that this paper holds its significance. This might also represent the first potential solution to Maxwell's demon problem<sup>9</sup>, proposed by James Clerk Maxwell in 1871.

To validate this concept, we begin by theoretically exploring how thermal energy can be converted into electrical energy. Our derivation shows that, during the acceleration process, the voltage difference induced by this phenomenon not only exists on the surface of the material but is also distributed evenly throughout the interior of the conductor. This finding offers new insight into the phenomenon of internal voltage differences and lays the foundation for future theoretical innovations.

Through theoretical derivation, we found that when the pH of an electrolyte is close to 7, even a small difference in ion concentration can cause significant changes in pH and chemical potential. In contrast, when the pH deviates significantly from 7, the same change in ion concentration results in only small changes in pH and chemical potential. This characteristic leads to a nonlinear relationship between the gravitational force (or centrifugal force) and the resulting voltage difference when the pH is near 7. This insight provides an explanation for the observed nonlinear behavior in the experimental results, highlighting the sensitivity of the system under near-neutral pH conditions.

Additionally, theoretically, under specific conditions derived from our theoretical framework, an aqueous solution of hydrogen iodide (HI) can generate approximately 72 W of

electrical energy per cubic meter of structural material and electrolyte. Furthermore, we conducted experiments to measure stable, long-term current output. While the observed energy output is small, this initial validation demonstrates that, with appropriate engineering optimization, this method could lead to a thermoelectric conversion system with economic feasibility for specific applications.

Consider a rotating system: if the rotation speed is doubled, the centrifugal force increases fourfold, meaning that only a quarter of the original distance is required to generate the same voltage difference. By connecting four such systems in series, the total voltage difference could reach four times the original value. Given that the resistance of the conductor is proportional to its thickness under the same cross-sectional area, the resistance at a quarter of the original distance would be one-fourth of the original value. Thus, the energy output from each system would be four times greater. The four systems can be placed in the same space. From this, it can be inferred that such a design could significantly increase the energy output efficiency by up to 16 times, whereas the air resistance energy consumption would only increase by approximately four times. Therefore, increasing the rotational speed could lead to the generation of practically usable electrical energy. In addition, there are many other ways to increase the output power, some of which are mentioned in the text.

In conclusion, while energy cannot be created from nothing, high-energy electrons are more likely to cross material interfaces in an accelerating field, facilitating current flow. As these high-energy electrons move through the material, the generation of electrical energy inevitably accompanies the dissipation of kinetic energy, akin to the dissipation of heat. Further theoretical development will explain how thermal vibrational energy drives charged particles to overcome gravitational or centrifugal forces, replenishing regions depleted by voltage differences or across

conductive interfaces. Since the system can maintain energy exchange under sustained acceleration, even in the absence of a temperature gradient, this process could transcend the limitations of the Carnot theorem, offering the potential to continuously convert ambient thermal energy into usable electrical energy. While my current study focuses on validating these observations experimentally, I acknowledge that future work should explore power output measurements.

## **2. MATERIALS AND METHODS**

To verify our hypothesis, we designed a structure resembling a battery in which positive and negative ions with different masses experience different forces in a centrifugal or gravitational field. This results in a potential difference at the terminals, and we measured whether this potential difference could provide a stable and long-term energy output. The fabrication and testing of the gravity battery involved several key steps, with each main experimental stage detailing the materials and equipment used, along with the rationale behind their selection.

1. *Electrode Preparation:* A titanium electrode plate (1 mm thick, 99.5% pure) was selected for its stability and was coated with a 1  $\mu\text{m}$  thick layer of platinum on both sides through electroplating. This platinum coating not only minimizes potential differences but also renders the electrode inert, significantly reducing the likelihood of chemical reactions with the electrolyte in the gravity battery. The platinum-coated titanium sheet was then cut into circular electrodes with a diameter of 50 mm via a water jet to ensure low temperatures during the cutting

process, thereby preserving the physical and chemical properties of the electrode surface.

2. *Cavity Formation:* Multiple silicone sheets, each with an outer diameter of 60 mm and an inner diameter of 40 mm, were used to form cavities for the gravity battery units. Silicone was chosen as the cavity material because of its chemical inertness, which prevents any reaction with ions in the electrolyte.
3. *Electrolyte Solution:* A potassium chloride solution (99.9% pure) was prepared with the pH adjusted to near neutrality ( $\text{pH} \approx 7$ ) to serve as the electrolyte. Potassium chloride was selected because the net weights of chloride and potassium ions in water, after accounting for buoyancy, significantly differ, enhancing the system's response. Additionally, setting the pH close to 7 allows for achieving the maximum potential difference with minimal ion concentration changes. These aspects will be discussed in detail later in the article.
4. *Battery Assembly:* The materials described above were used to assemble two gravity battery packs, each consisting of six small gravity cells electrically connected in series. The electrode spacings within the cells were set at 2 mm, 4 mm, 8 mm, 16 mm, 24 mm, and 32 mm. Arranging multiple cells with varying electrode spacings allows any significant reaction in one of the cells to be easily detected and measured, ensuring reliable data collection across different spacing conditions.
5. *External Connections and Housing:* Copper sheets (99% pure) were employed for external electrical connections because of their relatively low resistance, which helps minimize measurement deviations caused by external resistance and



improves overall measurement accuracy. The assembled gravity battery was housed in a 304 stainless steel casing and sealed with epoxy resin to ensure stability during testing. Stainless steel was chosen for its high strength and chemical inertness, preventing deformation under high gravity or centrifugal forces and ensuring that it would not corrode or degrade over prolonged measurements.

6. *Centrifuge Testing Setup:* The battery pack was placed in a centrifuge with a rotation radius of 1200 mm, and the centrifuge was accelerated to generate a centrifugal force equivalent to 10 times the gravitational force at the Earth's surface (10G). The large rotation radius was selected to ensure that the direction of the centrifugal force remained precisely vertical across different parts of the electrodes, whereas high acceleration was chosen to amplify the voltage, making it easier to measure.
7. *Voltage Measurement During Centrifugation:* Voltage and time data were recorded via an MMV-387SD three-channel voltage data recorder (Lutron, Sunwe Co., Taiwan) with a resolution of 0.1 mV.
8. *Long-term Stability Test:* The gravity battery was oriented in a forward position, ensuring the electrode surfaces were perpendicular to the direction of gravity. An external output impedance of 6.8 M $\Omega$  was connected, and the system was monitored over a period of 55 days. This setup aimed to verify that the generated voltage could persist over an extended duration with power output, confirming that it was not merely a transient phenomenon. The entire experiment was conducted in a room with a day-night temperature variation of less than 1.5°C,

and the sample was placed in an iron enclosure to ensure no electromagnetic interference and no uneven temperatures caused by air convection." Voltage measurements were taken via a Keysight 34465A digital multimeter (Keysight Technologies, Santa Rosa, CA, United States) with a resolution of 0.1  $\mu\text{V}$ .

9. *Inverted Position Test:* The gravity battery was then inverted (placed upside down) and subjected to a similar long-term test over 86 days, with voltage readings taken via the same Keysight multimeter setup. This was done to confirm that the voltage was indeed caused by gravitational acceleration, with the hypothesis that reversing the direction of gravity would result in an opposite voltage. Therefore, the sample was inverted for measurement.

## 2.1. Theoretical derivation process

### 2.1.1. Self-Generated Potential Difference of Plasma in a Gravity Field

The phenomenon of decreasing air density with increasing altitude on the Earth's surface is well known. Therefore, for a simple composition of gases, the concentration at higher altitudes is lower than that at lower altitudes. Specifically, the variation in the concentration of a pure gas with height, when in equilibrium, follows the Boltzmann distribution.<sup>10</sup> The relationship is described by Equation (1).

$$\frac{C_{h+\Delta h}}{C_h} = e^{-\frac{\varepsilon_{h+\Delta h} - \varepsilon_h}{kT}} = e^{-\frac{mG\Delta h}{kT}} \dots \dots \dots \quad (1)$$

where  $h$  is the height coordinate value,  $C_h$  is the concentration of ions at height  $h$ ,  $C_{h+\Delta h}$  is the concentration of ions at height  $h + \Delta h$ ,  $\varepsilon_h$  is the potential energy of the ion at height  $h$ ,  $\varepsilon_{h+\Delta h}$  is

the potential energy of the ion at height  $h + \Delta h$ ,  $m$  is the mass of the particle (or ion),  $G$  is gravity,  $mG$  is the gravitational force on the particle (or ion), and  $kT$  is the product of the Boltzmann constant  $k = 1.380649 \times 10^{-23} \text{ J/K}^{11}$  and the thermodynamic temperature  $T$ .

Applying the same principle, considering a plasma medium that is either fully ionized or nearly fully ionized, in the presence of gravity but in the absence of an electric field, when in equilibrium, the distribution of ions inside the plasma with height will be as shown in Equation (2).

$$\frac{C_{h+\Delta h}}{C_h} \Big|_{E=0} = e^{-\frac{\varepsilon_{h+\Delta h} - \varepsilon_h}{kT}} \Big|_{E=0} = e^{-\frac{mG\Delta h}{kT}} \Big|_{E=0} \dots \dots \dots \quad (2)$$

where  $E$  is the electric field.

Notably, Equations (1) and (2) contain a mass variable  $m$ , meaning that heavier particles will experience a greater change in concentration with height than lighter particles. Thus, in the absence of an electric field, ions with larger masses are subjected to greater gravitational forces, resulting in a larger concentration difference between high and low positions. In contrast, in the absence of an electric field, ions with smaller masses experience weaker gravitational forces, leading to a smaller concentration difference. Therefore, as seen from Equation (2), in the absence of an electric field and when the masses of positive and negative ions in the plasma are different, the lower region will have a greater number of heavier ions than lighter ions, whereas the upper region will have a greater number of lighter ions than heavier ions. For example, in  $Li^+$  and  $Cl^-$  plasmas, the mass of  $Cl^-$  is approximately 5 times greater than that of  $Li^+$ , so the gravitational force of  $Cl^-$  is also approximately 5 times greater than that of  $Li^+$ . When the number of positive and negative ions is the same, on the basis of equation (2) and the abovementioned principles, in the absence of an electric field, the number of chloride ions  $Cl^-$  will be greater than the number of lithium ions  $Li^+$  in the lower region of the plasma, resulting in

a negative charge. In the upper region, the number of chloride ions  $Cl^-$  is less than that of lithium ions  $Li^+$ , resulting in a positive charge. When the electricity above the plasma is positive and the electricity below it is negative, a top-down electric field is generated. This electric field causes  $Cl^-$  to move upward and  $Li^+$  to move downward, reducing the difference in charge between the upper and lower parts. The rates of change of positive ions and negative ions in the plasma change with height are the same on the basis of charge balance. That is, when charge balance is achieved, apart from the uppermost and lowermost regions, the intermediate area remains electrically neutral. In the case of charge balance, when the residual electric field strength is  $E$ , equation (3) can be obtained by adding the electric field term  $E$  to the Boltzmann distribution<sup>10</sup> in equation (2), and equation (4) can be derived from equation (3):

$$\frac{C_{Li^+(h+\Delta h)}}{C_{Li^+(h)}} = e^{-\frac{(m_{Li^+}G+qE)\Delta h}{kT}} = \frac{C_{Cl^-(h+\Delta h)}}{C_{Cl^-(h)}} = e^{-\frac{(m_{Cl^-}G-qE)\Delta h}{kT}} \quad \dots \dots \dots \quad (3)$$

$$m_{Li^+}G + qE = m_{Cl^-}G - qE$$

$$E = \frac{(m_{Cl^-}-m_{Li^+})G}{2q} \quad \dots \dots \dots \quad (4)$$

where  $C_{Li^+(h)}$  is the concentration of  $Li^+$  at height  $h$ ,  $C_{Li^+(h+\Delta h)}$  is the concentration of  $Li^+$ s at height  $h + \Delta h$ ,  $m_{Li^+}$  is the mass of  $Li^+$ ,  $E$  is the electric field inside the plasma and is positive in the downward direction,  $G$  is gravity and is positive in the downward direction,  $C_{Cl^-(h)}$  is the concentration of  $Cl^-$  at height  $h$ ,  $C_{Cl^-(h+\Delta h)}$  is the concentration of  $Cl^-$ s at height  $h + \Delta h$ ,  $m_{Cl^-}$  is the mass of  $Cl^-$ , and  $q$  represents the charge of the negative electron, which is

$$1.602176634 \times 10^{-19}C. \quad ^{11}$$

Importantly, the electric field in equation (4) exists within the plasma body. This means that charge accumulation occurs at the upper and lower surfaces and that there is no charge accumulation inside the plasma; however, an electric field is distributed throughout the entire

plasma body rather than being confined to its surface. In other words, gravity or a centrifugal force generates an electric field within the conductor (plasma).

Another noteworthy point is that Tolman's 1910 experiment demonstrated that increasing the concentration of iodide ions had a minimal effect on the voltage generated in a centrifugal field. This aligns with our derived Equation (4), which indicates that the electric field in plasmas or conductors depends solely on the individual masses of the ions <sup>4</sup> and is independent of the ion concentration.

When the height difference from top to bottom is H, the voltage difference  $\nabla V$  can be obtained as shown in equation (5):

$$\nabla V = \frac{(m_{Cl^-} - m_{Li^+})GH}{2q} \dots \dots \dots \quad (5)$$

Equations (4) and (5) indicate that whenever the masses of the positive and negative charge carriers in the plasma are different, an electric field will spontaneously form inside the plasma body under the influence of gravitational or centrifugal forces. This extends the effect of acceleration forces, causing internal voltage differences<sup>4</sup> by expanding the electric field from the surface of the conductor to its interior.

*2.1.2. Illustrate the energy conversion mechanism*

Currently, the plasma formed by lithium ions and electrons is widely used in many applications. Using the same derivation and calculations, equation (4) can be expanded to equation (6):

$$E = \frac{(m_- - m_+)G}{2q} \dots \dots \dots \quad (6)$$

where  $m_+$  represents the mass of positively charged particles in the plasma and where  $m_-$  represents the mass of negatively charged particles. In lithium plasma, the positively charged

particles are lithium ions with a mass of  $1.157 \times 10^{-26}\text{kg}^{12}$ , whereas the negatively charged particles are electrons with a mass of  $9.109 \times 10^{-31}\text{kg}^{13}$ . Since the mass of lithium ions is significantly greater than that of electrons, equation (6) can be simplified to equation (7).

$$E_{in.Li+.plasma} \cong -\frac{m_{Li+G}}{2q} \dots \dots \dots \quad (7)$$

Equation (7) shows that owing to the mass difference between lithium ions and electrons, the electric field required to maintain plasma neutrality is not zero. This means that in the presence of a gravitational or centrifugal field, a nonzero electric field exists within the lithium plasma. Next, by considering a plasma formed by potassium ions and electrons and following the same approach as in the previous example with lithium ions, we obtain equation (8).

$$E_{in.K+.plasma} \cong -\frac{m_{K+G}}{2q} \dots \dots \dots \quad (8)$$

Notably, when equations (7) and (8) are compared, the mass of potassium ions, approximately  $6.492 \times 10^{-26}\text{kg}^{12}$ , is much greater than that of lithium ions, which is  $1.157 \times 10^{-26}\text{kg}^{12}$ . This causes the electric field formed within the potassium ion plasma in the same gravitational or centrifugal field to be significantly stronger than that formed within the lithium ion plasma. This also leads to a much greater potential change within the potassium-ion plasma than in the lithium-ion plasma over the same distance along the direction of the force field. Consider the structure shown in Fig. 1. On the left is a chamber with lithium ion plasma in an insulator, and on the right is a chamber with potassium ion plasma in an insulator. Each chamber is connected by a conductor at a height difference of  $h$ . From the previous derivation, we know that because the electric fields in the two plasmas differ under gravity, the potential differences at the same height also differ. If the voltage difference between the conductor ends below is zero, we can find the potential difference of the upper conductor, as shown in equation (9).

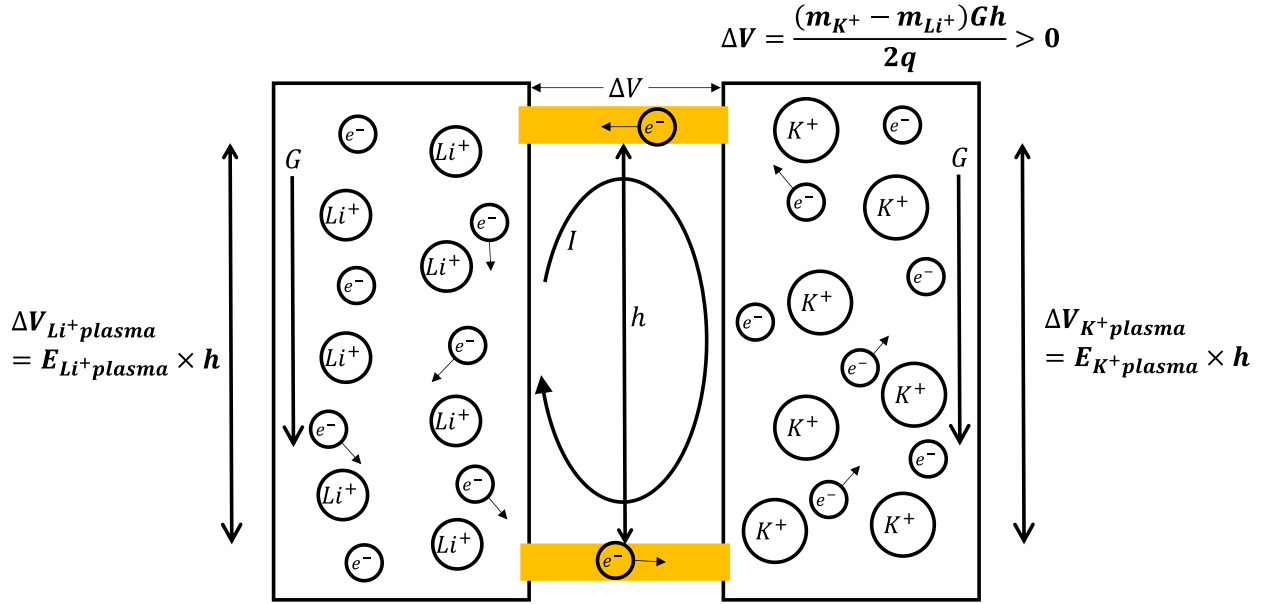


**Fig. 1.** Two adjacent chambers are under the influence of a gravitational field, with one containing lithium-ion plasma and the other containing potassium-ion plasma. Electrical connections are made at the top and bottom of each chamber, showing a schematic representation of the spontaneously generated current within the system.

$$\Delta V = E_{Li^+plasma} \times h - E_{K^+plasma} \times h = \frac{(m_{K^+} - m_{Li^+})Gh}{2q} > 0 \dots \dots \dots (9)$$

Equation (9) shows that because the masses of potassium ions and lithium ions are different, a potential difference forms across the upper conductor. The voltage on the side near the lithium plasma is higher than that near the potassium plasma. When a potential difference forms across the conductor, a spontaneous current flows to balance it. This creates an electron flow from the potassium plasma to the lithium plasma, or equivalently, a current from the lithium plasma to the potassium plasma. Owing to this electron flow, the upper part of the potassium plasma loses electrons, lowering its concentration below equilibrium. This causes electrons in the potassium plasma to diffuse upward due to thermal motion. In the lithium-ion plasma, an electron

concentration higher than the equilibrium level in the upper region causes electrons to diffuse downward. On the basis of charge balance, spontaneous electron flow occurs from the lithium plasma to the potassium plasma in the lower conductor. Thus, a spontaneous circulating current forms in this structure, following the clockwise direction in the figure. Notably, the energy for this electron diffusion comes from thermal energy, whereas the circulating current is electrical energy. Thus, thermal energy is converted into electrical energy. In other words, two parallel, different plasma bodies spontaneously generate a circulating current that converts thermal energy into electrical energy. This heat-to-electricity conversion without a temperature difference goes beyond the Carnot Theorem<sup>1</sup> (published by Nicolas Léonard Sadi Carnot in 1820). It surpasses the second law of thermodynamics<sup>2</sup>.

### *2.1.3. A Hypothetical Process Similar to Maxwell's Demon for Understanding the Phenomenon of Gravity-Induced Thermoelectric Conversion*

As shown in Figure 2-(a), there are two plasma regions: one containing potassium ions and the other containing lithium ions. When the two plasmas remain independent without exchanging ions or electrons, in equilibrium, heavier gas molecules tend to accumulate near the ground, whereas lighter gas molecules exhibit little concentration difference between high and low altitudes. The heavier potassium ions experience a stronger downward gravitational force and thus concentrate more at the lower end. In contrast, the lighter lithium ions, which have a weaker gravitational pull, show negligible downward concentration tendencies, which can be initially disregarded. Electrons, driven by thermal vibrations, diffuse upward more readily than positive ions do. Consequently, the lower portion of the potassium plasma becomes slightly



positively charged because of the higher concentration of positive ions, whereas the upper portion becomes negatively charged. This phenomenon is less pronounced in lithium plasma.

If a small hole is drilled as the aperture at both the top and bottom where the two plasmas are separated, as shown in Figure 2-(b), allowing only electrons to pass while blocking ions, an imbalance spontaneously arises. To maintain the reversibility of the electron pathways, the apertures from both plasma sides are identical. At the upper aperture, the potassium plasma, which is negatively charged, accelerates electron transport toward the lithium plasma, increasing the likelihood of passing through it. Conversely, electrons traveling from the lithium plasma toward this aperture are repelled by its negative charge and are more likely to be deflected back into the lithium plasma. As a result, more electrons flow through the aperture from the potassium plasma to the lithium plasma than in the reverse direction. A similar principle applies to the lower aperture but in the opposite direction: electrons from the potassium plasma are attracted back by the positive charge, resulting in fewer electrons passing through to the lithium plasma than in the reverse direction.

This creates an imbalance: at the upper end, the electron concentration in the potassium plasma decreases, deviating from equilibrium, whereas the electron concentration in the lithium plasma increases, also deviating from equilibrium. Conversely, at the lower end, the electron concentration in the potassium plasma increases, whereas that in the lithium plasma decreases. Both plasmas are also out of equilibrium at the lower end. Driven by the energy of thermal vibrations, particles diffuse and flow toward equilibrium. This diffusion phenomenon generates an upward net electron flow in the potassium plasma and a downward net electron flow in the lithium plasma. In the structure shown in Figure 2-(b), these flows form a counterclockwise

electron loop, corresponding to a clockwise electric current. This process resembles Maxwell's hypothetical demon.

Therefore, in such a structure, as long as thermal vibrations and gravity coexist, a net electron flow is generated. This electron flow can be utilized to convert thermal energy into electrical energy without a temperature gradient.

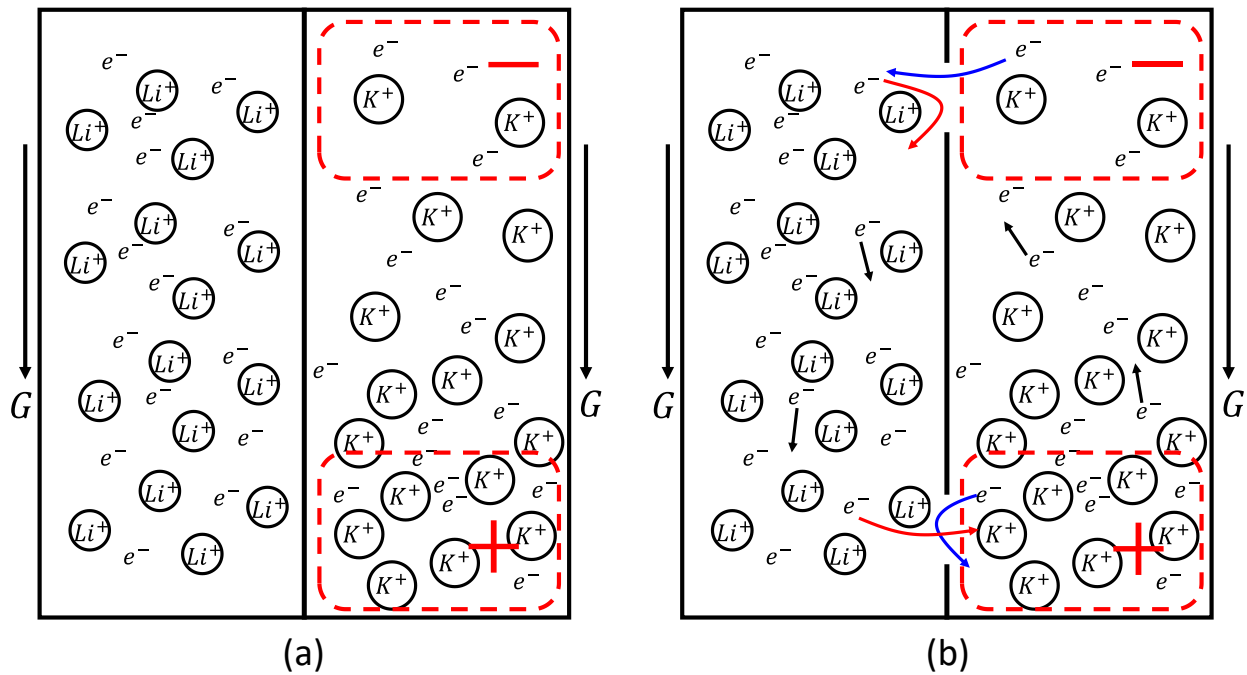


**Fig. 2.** Illustrates the concept via an approach similar to Maxwell's reasoning. (a) Two adjacent plasma bodies are shown, one being a potassium ion plasma and the other being a lithium ion plasma. Each plasma is treated as independent, with the potassium ion plasma exhibiting a more pronounced potential difference, showing negative bias at the upper region and positive bias at the lower region. In contrast, the lithium-ion plasma has minimal and less noticeable potential deviation. (b) Small openings are introduced at both the upper and lower regions of the two plasma bodies. At the upper opening, the negatively biased potassium ion plasma repels electrons coming from the lithium ion plasma, causing these electrons to be more likely to move

back toward the lithium ion plasma owing to the repulsive force. At lower openings, the positively biased potassium ion plasma has the opposite effect, attracting electrons from the lithium ion plasma.

#### *2.1.4. Electric Field Formation and Voltage Difference Across Ionic Aqueous Solutions in a Gravity Field*

The previous paragraph used plasma as a theoretical deduction. However, ion plasma requires high temperatures and is difficult to control and operate; however, at normal temperatures, ions can be found in aqueous solutions. Considering an ionic aqueous solution, when the net masses or mass–charge ratios of positive and negative ions in water (the weight of the ions minus the buoyancy force of the water on the ions) are different, a potential difference can also be generated by gravity. As demonstrated in Tolman's 1910 experiment, the offset voltage of a lithium iodide aqueous solution under a specific rotational speed (approximately 70 units) was approximately  $4.3 \text{ mV}^4$ , whereas the offset voltage of a potassium iodide aqueous solution under the same rotational speed (and thus the same centrifugal force) was approximately  $3.5 \text{ mV}^4$ , indicating a significant difference.

If a setup similar to that in Fig. 1 is used, with one side replaced by a lithium iodide aqueous solution instead of lithium plasma and the other side replaced by a potassium iodide aqueous solution instead of potassium plasma, a similar voltage difference and thermoelectric conversion effect can be achieved.

Next, we employ a configuration in which one side is an aqueous electrolyte solution and the other side is a copper conductive plate as the basis for calculations and experiments. As Tolman mentioned in his 1916 paper, the offset voltage in metals under the same acceleration is

significantly smaller than that in ionic liquids <sup>5</sup>, suggesting that a similar effect should also be achievable.

### 2.1.5. Estimation of Output Energy Using Hydrogen Iodide as an Example

To estimate the potential energy output, we consider an aqueous solution of hydrogen iodide. In Figure 3, the gray region represents a high-strength aluminum alloy, which is assumed to have a yield strength of  $Y=670$  MPa. The blue region represents the electrolyte solution, which consists of hydrogen iodide in water. The distance from the center of the large circular disk to the center of the cross-section of the annular electrolyte is denoted as  $r_3$ . The cross-sectional radius of the electrolyte solution is  $r_1$ , whereas the outer radius of the cross-sectional hollow annular structure containing the electrolyte is  $r_2$ . The aluminum alloy disk has a thickness  $d$  of approximately  $r_3 - r_2$  from the disk center.

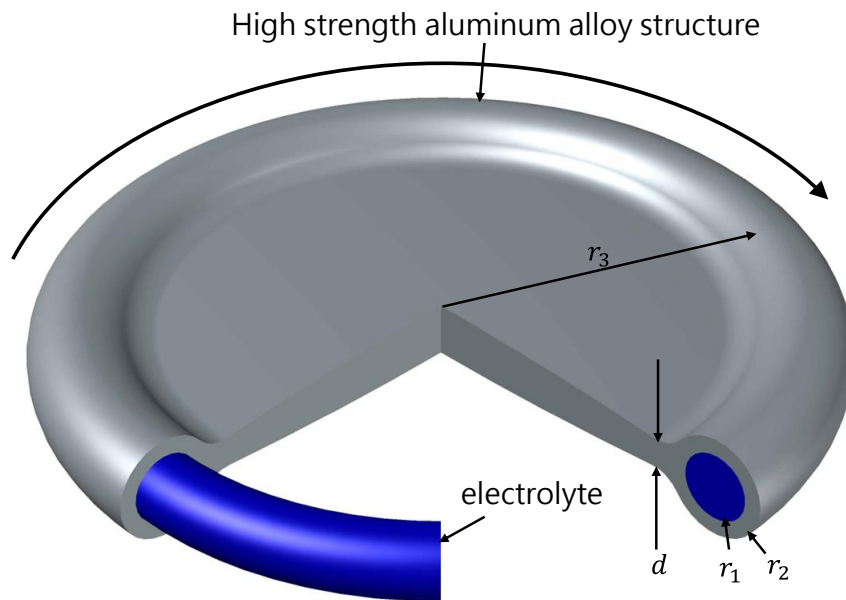


**Fig. 3.** Illustrates the structural configuration and dimensional notations used for simulating the maximum electrical power output

At a rotational speed  $\omega$ , the centrifugal force per unit volume of the electrolyte is approximately  $\rho_{liquid} \times r_3 \times \omega^2$ , where  $\rho_{liquid}$  is the density of the electrolyte solution. Consequently, the centrifugal force on the electrolyte per unit length along the radius  $r_3$  is  $\pi \times r_1^2 \times \rho_{liquid} \times r_3 \times \omega^2$ . The hollow annular aluminum alloy structure along the radius  $r_3$  experiences a centrifugal force per unit length of  $\pi \times (r_2^2 - r_1^2) \times \rho_{solid} \times r_3 \times \omega^2$ , where  $\rho_{solid}$  is the density of the high-strength aluminum alloy. Assuming that the centrifugal force is fully supported by the tensile strength of the annular structure along  $r_3$ , the maximum tolerable rotational speed  $\omega_1$  can be derived, resulting in Equation (10).

$$\begin{aligned} \pi(r_2^2 - r_1^2)Y &= (\pi\rho_{solid}(r_2^2 - r_1^2)r_3\omega_1^2 + \pi\rho_{liquid}r_1^2r_3\omega_1^2)r_3 \\ \Rightarrow \omega_1^2 &= \frac{(r_2^2 - r_1^2)Y}{r_3^2(\rho_{solid}(r_2^2 - r_1^2) + \rho_{liquid}r_1^2)} \quad \dots \dots \dots (10) \end{aligned}$$

Alternatively, assuming that the centrifugal force is entirely supported by the inward tensile force of the disk, the maximum tolerable rotational speed  $\omega_2$  directed toward the center can be derived, resulting in Equation (11).

$$\begin{aligned} Yd \frac{r_3 - r_1}{r_3} &= \pi\rho_{solid}(r_2^2 - r_1^2)r_3\omega_2^2 + \pi\rho_{liquid}r_1^2r_3\omega_2^2 \\ \Rightarrow \omega_2^2 &= \frac{Y(r_3 - r_1)d}{\pi r_3^2(\rho_{solid}(r_2^2 - r_1^2) + \rho_{liquid}r_1^2)} \quad \dots \dots \dots (11) \end{aligned}$$

When both the tensile force in the annular structure and the inward tensile force act simultaneously, the maximum tolerable rotational speed  $\omega_3$  can be derived by combining Equations (10) and (11), resulting in Equation (12).

$$\omega_3^2 = \omega_1^2 + \omega_2^2 = \frac{[(r_2^2 - r_1^2) + (r_3 - r_1)d]Y}{r_3^2(\rho_{solid}(r_2^2 - r_1^2) + \rho_{liquid}r_1^2)} \quad \dots \dots \dots (12)$$

By selecting parameters  $r_1 = 0.0025$  m,  $r_2 = 0.00355$  m,  $r_3 = 0.005$  m,  $d = 0.0021$  m,  $\rho_{solid} = 2700$  kg/m<sup>3</sup>, and  $\rho_{liquid} = 1000$  kg/m<sup>3</sup>, substitution into Equation (12) yields  $\omega_3^2 = 9.1888 \times 10^9$  sec<sup>-2</sup>. The maximum acceleration experienced by the electrolyte solution can then be calculated as  $\omega_3^2 r_3 \cong 4.5944 \times 10^7$  m/sec<sup>2</sup>. In solution, both the iodide anions and hydrogen cations are subjected to the same acceleration. Owing to the large mass of iodide ions, the buoyant force in water is negligible. Similarly, the buoyant force on hydrogen ions, with their small volume, can also be neglected. Using the approximate calculation method from Equation (6), the resulting electric field is estimated to be 29.97 V/m. Here, the mass of the iodide ion is approximately  $2.1073 \times 10^{-25}$  kg<sup>12,13</sup>, the mass of the hydrogen ion is  $1.1526 \times 10^{-26}$  kg<sup>12,13</sup>, and the elementary charge is  $-1.602 \times 10^{-19}$  C<sup>11</sup>. The conductivity of the hydrogen iodide solution can be adjusted to 0.85 S/m<sup>14</sup>, resulting in a resistance of approximately 1.1765  $\Omega$  for a 1 m<sup>3</sup> cube. Assuming that the maximum output voltage drop is half the maximum voltage, the energy output of the cube can be estimated as  $(29.97/2)^2 / 1.1765$  W. In addition to the effects of the annular structure, the energy output per unit volume of 1 m<sup>3</sup> is approximately 72 W. This energy density falls within an acceptable range for power generation applications. Some other conditions are listed in Table 1.

Parameter	$r_1 = 0.0025$ m	$r_1 = 0.01$ m	$r_1 = 0.04$ m
$r_2$ (m)	0.00355	0.0142	0.0568
$r_3$ (m)	0.005	0.02	0.08
$d$ (m)	0.0021	0.0084	0.0336
$\rho_{solid}$ (kg/m <sup>3</sup> )	2700	2700	2700
$\rho_{liquid}$ (kg/m <sup>3</sup> )	1000	1000	1000
$m_{H^+}$ (kg) <sup>12,13</sup>	$1.1526 \times 10^{-26}$	$1.1526 \times 10^{-26}$	$1.1526 \times 10^{-26}$
$m_{I^-}$ (kg) <sup>12,13</sup>	$2.1073 \times 10^{-25}$	$2.1073 \times 10^{-25}$	$2.1073 \times 10^{-25}$
Y (MPa)	670	670	670

$\omega_1^2$ ( $sec^{-2}$ )	$7.275 \times 10^9$	$4.547 \times 10^8$	$2.842 \times 10^7$
$\omega_2^2$ ( $sec^{-2}$ )	$1.914 \times 10^9$	$1.196 \times 10^8$	$7.476 \times 10^6$
$\omega_3^2$ ( $sec^{-2}$ )	$9.189 \times 10^9$	$5.743 \times 10^8$	$3.589 \times 10^7$
$a$ ( $m/sec^{-2}$ )	$4.594 \times 10^7$	$1.1486 \times 10^7$	$2.872 \times 10^6$
$E$ ( $V/m$ )	29.97	7.494	1.8734
Conductivity (S/m)	0.85	0.85	0.85
$P_{liquid}/m^3$ (W/m <sup>3</sup> )	190.92	11.933	0.7458
$P_{solid+liquid}/m^3$ (W/m <sup>3</sup> )	72.23	4.514	0.2821

**Table 1.** The simulation results for the output power of a hydrogen iodide solution were calculated for selected cross-sectional radii of the electrolyte ring at 0.0025 m, 0.01 m, and 0.04 m.

#### 2.1.6. Selection of Experimental Conditions Based on the Principle of Significant Voltage Variation from Small Ion Concentration Changes in Strongly Electrolyte Solutions at Near-Neutral pH

From the previous derivations and calculations, it is evident that achieving significant voltage changes requires extremely strong centrifugal forces, making experimental measurements challenging. However, chemical titration experiments have demonstrated that in strong electrolyte aqueous solutions, even minimal changes in ion concentration can result in substantial pH variations. These pH changes can be measured as potential differences via a pH meter.

Practically, this principle can be leveraged to amplify voltage differences and increase energy output, although further experiments are necessary to verify the specific conditions and effects. When the pH is close to 7, small changes in the ion concentration can lead to significant variations in the potential. Conversely, when the pH deviates significantly from neutrality—

becoming either higher or lower—the same changes in ion concentration result in much smaller potential variations. This finding indicates that the relationship between the voltage change and the centrifugal force exhibits nonlinear characteristics when the pH approaches neutrality (approximately 7).

To facilitate observation and measurement, we selected a potassium chloride aqueous solution as the experimental medium for this study. Because chloride ions and potassium ions are both strong electrolytes, they are almost completely dissociated. Owing to the effect of gravity, the potential energy of the ions changes, causing the ion concentration to change with height. The concentrations of chloride ions and potassium ions change with height due to the potential energy difference caused by gravity. According to Boltzmann's distribution law,<sup>10</sup> the concentration changes with height in the steady state without convection can be obtained as shown in equations (13) and (14):

$$[C_{K^+}]_h = [C_{K^+}]_0 e^{-\frac{m_{K^+.net} Gh}{kT}} \quad \dots \dots \dots \quad (13)$$

$$[C_{Cl^-}]_h = [C_{Cl^-}]_0 e^{-\frac{m_{Cl^-.net} Gh}{kT}} \quad \dots \dots \dots \quad (14)$$

where  $h$  is the height coordinate value,  $[C_{K^+}]_h$  is the potassium ion concentration at height  $h$ ,  $[C_{K^+}]_0$  is the potassium ion concentration at height 0,  $m_{K^+.net}$  is the net effective mass of potassium ions after accounting for buoyant force in water,  $[C_{Cl^-}]_h$  is the chloride ion concentration at height  $h$ ,  $[C_{Cl^-}]_0$  is the chloride ion concentration at height 0, and  $m_{Cl^-.net}$  is the net effective mass of chloride ions after accounting for buoyant force in water.

When calculating the net mass of an ion, the buoyant force exerted by water on the ion must be subtracted from the mass of the ion, as the densities of potassium ions and chloride ions are relatively close to those of water molecules, making the buoyant force significant and unable to be ignored. To determine this buoyant force, the effective volume of the ion is first calculated.



This volume is then multiplied by the density of water to obtain the buoyant force acting on the ion. A KCl aqueous solution with a concentration of 2 N was used as an example.

On the basis of the density of HCl at a concentration of 2 N ( $1.03008 \text{ g/cm}^3$ )<sup>15</sup> and at a concentration of 1.8 N ( $1.02690 \text{ g/cm}^3$ )<sup>15</sup> and considering that the volume of hydrogen ions is negligible, the effective volume of chloride ions at a concentration close to 2 N is estimated to be approximately  $3.2928 \times 10^{-23} \text{ cm}^3$ . The net mass of chloride ions, after the buoyant force of water at this concentration is subtracted, is calculated to be approximately  $2.3252 \times 10^{-26} \text{ kg}$ .

Similarly, based on the density of KCl at a concentration of 2 N ( $1.08166 \text{ g/cm}^3$ )<sup>16</sup> and at a concentration of 1.8 N ( $1.07390 \text{ g/cm}^3$ )<sup>16</sup>, and utilizing the previously determined effective volume of chloride ions, the effective volume of potassium ions at a concentration close to 2 N was estimated to be approximately  $1.8608 \times 10^{-23} \text{ cm}^3$ . The net mass of potassium ions, after the buoyant force of water at this concentration is subtracted, is calculated to be approximately  $4.4797 \times 10^{-26} \text{ kg}$ .

Substituting the net masses of chloride and potassium ions into Equations (13) and (14), the variation in the chloride and potassium ion concentrations with height under an acceleration equivalent to Earth's gravitational acceleration (assuming equal concentrations of chloride and potassium ions at the reference height) is shown in Figure 4.

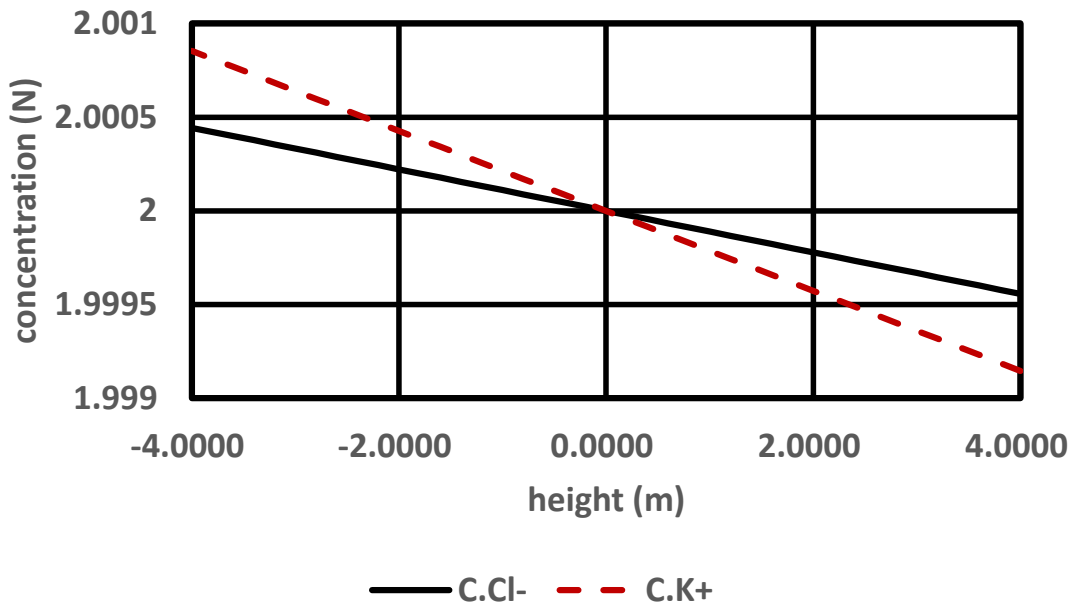
Since both potassium and chloride ions are strong electrolytes, they dissociate nearly completely in water. When chloride ions are more abundant than potassium ions are, the hydrogen ions that dissociate from water compensate to achieve electrical neutrality. Conversely, when chloride ions are less abundant than potassium ions are, hydroxide ions that dissociate from water compensate for the electrical balance. Using the fundamental laws of pH, the variation in pH with height can be determined and is shown in Figure 5.

By applying the Nernst equation (Equation (15))<sup>17</sup>, the voltage variation with height can be calculated. When the electrode primarily exchanges electrons with chloride ions, the voltage variation is represented by the solid line in Figure 6. When the electrode primarily exchanges electrons with potassium ions, the voltage variation is represented by the dashed line in Figure 6. If the electrode primarily exchanges electrons with hydrogen ions or hydroxide ions, the voltage variation with height is shown as the solid line in Figure 7.

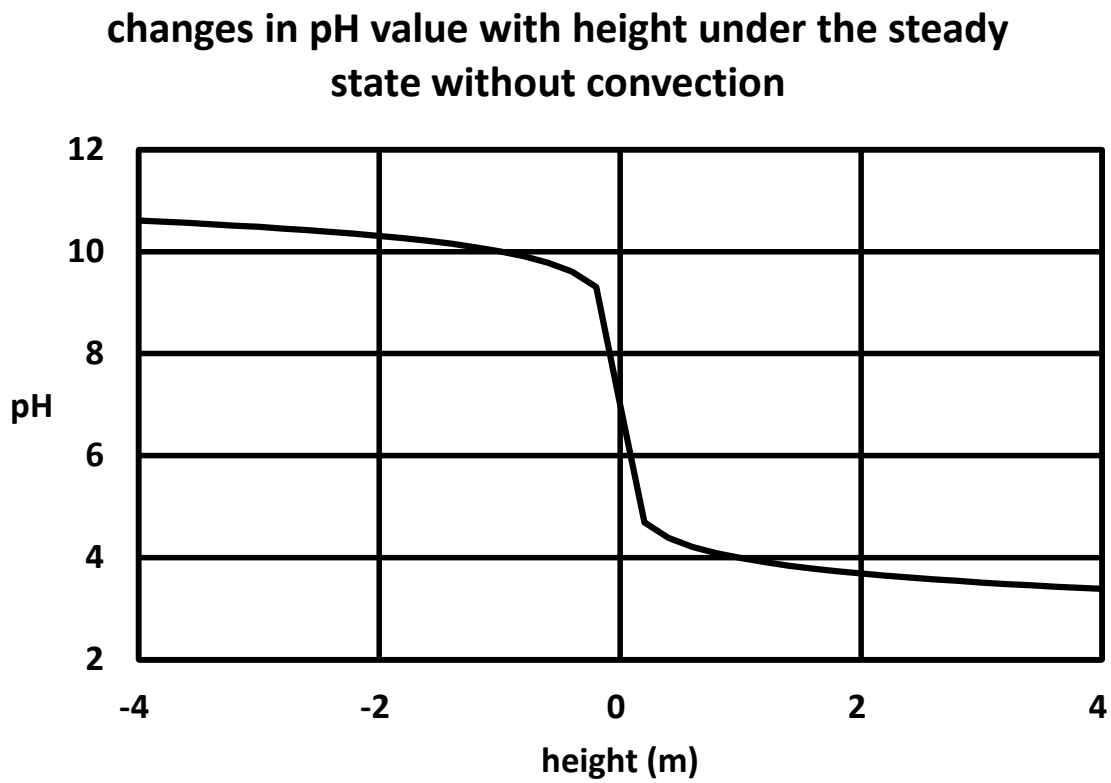
$$\Delta V = -\frac{RT}{nF} \ln\left(\frac{[C]}{[C]_0}\right) \quad \dots \dots \dots \quad (15)$$

Figure 7 also reveals that when the electrode exchanges electrons primarily with hydrogen ions or hydroxide ions, the voltage variation with height is nonlinear. This nonlinear behavior can explain the phenomena observed in our experiments.

**changes in chloride ion concentration and potassium ion concentration with height under the steady state without convection**



**Fig. 4.** The concentrations of chloride ions and potassium ions at zero height are both 2 N, and the changes in the chloride ion concentration and potassium ion concentration with height are under the steady state without convection. The vertical axis is the concentration value in N, and the horizontal axis is the height value in m.



**Fig. 5.** The calculated pH value of the KCl aqueous solution at equilibrium. The vertical axis represents the pH value, and the horizontal axis represents the height in m.

Potential changes with height when the electrode exchanges electrons with chloride ions and exchanges electrons with potassium ions

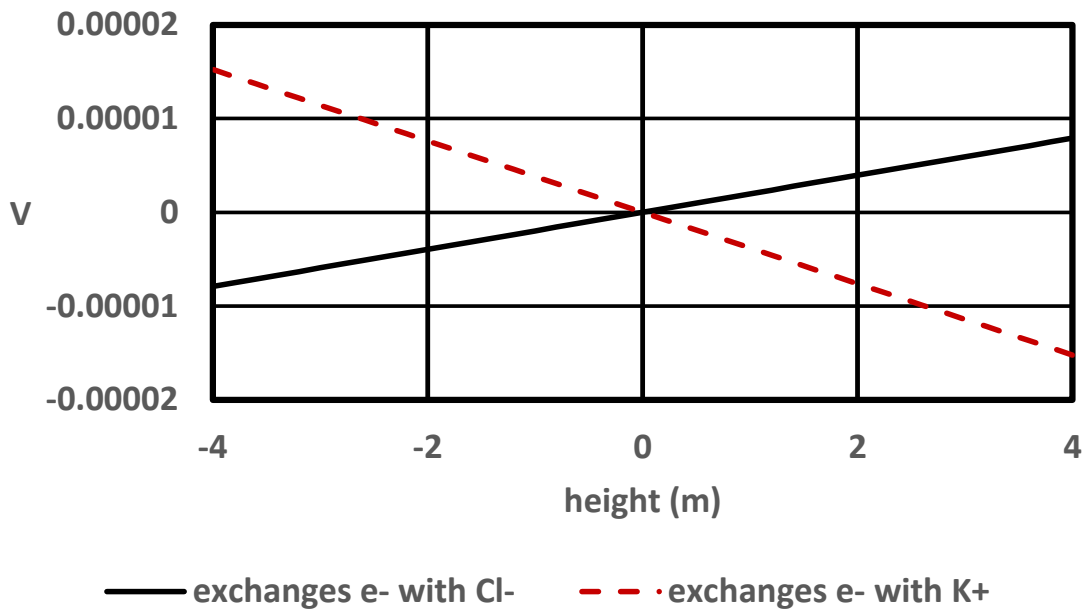


**Fig. 6.** The potential changes with height when the electrode exchanges electrons with chloride ions and exchanges electrons with potassium ions.

### The change in potential with height when the electrode exchanges electrons with hydrogen ions or hydroxide ions

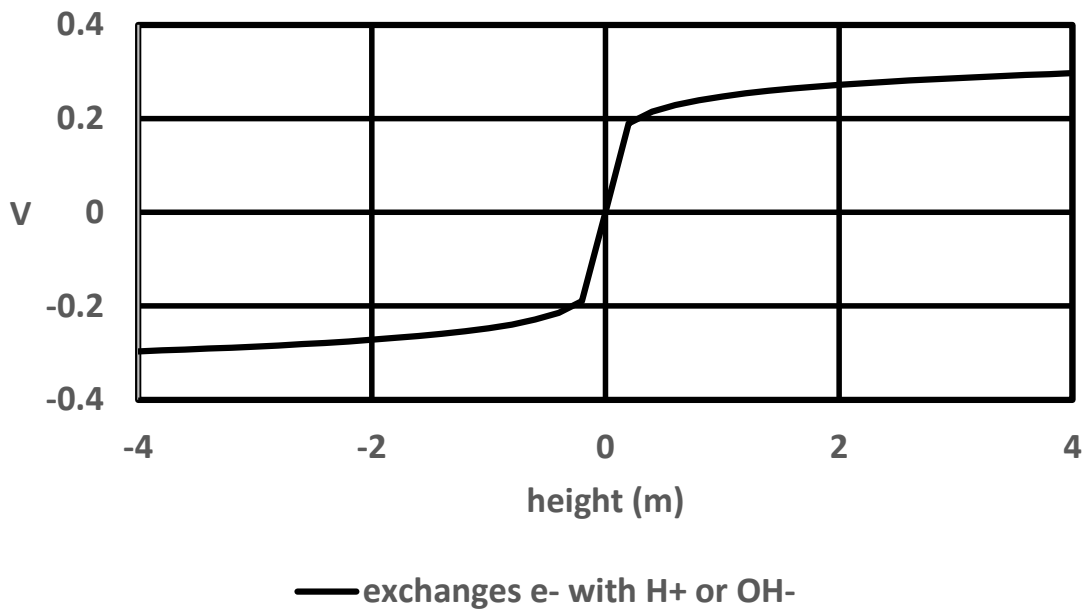


**Fig. 7.** The change in potential with height when the electrode exchanges electrons with hydrogen ions or hydroxide ions.

The lower the pH is, the higher the concentration of hydrogen ions, and the opposite is true for hydroxide ions. Fig. 5 shows that the concentration of hydrogen ions is greater at high positions, and the concentration of hydroxide ions is greater at low positions. When the upper and lower ends are connected to a resistor, the resistor links the two ends, altering the voltage and causing the ion concentrations to deviate from equilibrium, thus initiating diffusion. In this process, the hydrogen ions above diffuse downward, whereas the hydroxide ions diffuse upward, meeting and combining in the central area to form water. This is similar to what occurs in plasma, where the diffusion energy of atoms and ions is also derived from the thermal energy of thermal vibrations. The downward movement of positively charged hydrogen ions and the

upward movement of negatively charged hydroxide ions can both create internal currents from top to bottom, thus forming a gravity battery that outputs electrical energy through an external resistor. Similarly, when positively charged potassium ions and negatively charged chloride ions diffuse upward or downward, an electric current is also generated. Therefore, the energy is sent out without a temperature difference.

The above discussion theoretically examines the changes in concentration and electric field within plasma or ionic solutions under the influence of gravitational or centrifugal forces, essentially in the presence of acceleration. The following section describes our experimental approach to validate this phenomenon and how we measured continuous and stable current outputs in the absence of a temperature difference.

## **2.2. Experimental Verification**

### *2.2.1. Experimental Procedure*

To assess the impact of gravity on the ion concentration and electrical potential in potassium chloride (KCl) solutions, we designed a set of gravity cells using titanium electrode sheets coated with platinum. Titanium was chosen for its chemical inertness, preventing any unwanted reactions with the KCl solution. Each electrode sheet had a diameter of 50 mm and was coated with 1  $\mu\text{m}$  of platinum on both sides.

Silicone rings, with an inner diameter of 40 mm and an outer diameter of 60 mm, were used to create cavities to hold the ionic aqueous solution. The silicone rings were carefully selected to avoid any chemical reactions with the solution. Each cavity was equipped with a silicone tube to facilitate filling with the KCl solution. The overall design of the cell, including

the assembly of multiple layers separated by silicone rings of varying thicknesses (2 mm to 32 mm), allowed for a series of electrical connections across the chambers. The arrangement is depicted in Figure 8.

The theoretical derivation suggested that the largest voltage change occurs when the pH is close to 7. Therefore, a 2 N KCl aqueous solution with a pH near 7 was prepared through vacuum degassing, which minimizes gas bubbles that could otherwise obstruct potential conduction or current flow. However, vacuum degassing also poses the risk of altering the pH by removing trace amounts of chlorine gas. Two gravity cells with different degassing durations were prepared. The longer degassing time of one cell led to a slight reduction in the chloride ion concentration due to chlorine gas removal.

Once prepared, the degassed KCl solution was injected into each cavity of the gravity cells, and the openings were sealed. The electrode connections were then completed, as shown in the center panel of Figure 8, with the internal structure displayed in Figure 9. Epoxy resin was used to seal the assembled cells within stainless steel casings to prevent deformation or leakage during high-centrifugal force experiments.

The gravity cells were placed into a centrifuge with a rotation radius of 1200 mm and balanced by placing them opposite one another to maintain a stable center of gravity. The experimental setup included an MMV-387SD voltage recorder positioned at the center of the centrifuge. The centrifuge was operated at 10 G (ten times Earth's gravity) for two hours, during which the voltage output was continuously monitored. This duration allowed sufficient diffusion time for the solution to reach a near-equilibrium ion concentration gradient, confirming that a voltage difference can be generated under high centrifugal force.

After the centrifugal force measurements, the cells were allowed to rest for 30 minutes, during which the discharge process was recorded, demonstrating that the voltage difference disappears once the centrifugal force is removed.

To fully discharge the gravity cells and remove any residual charge, they were short-circuited and left horizontally for 290 days (with gravity parallel to the electrode plates). The samples were subsequently placed vertically (gravity perpendicular to the electrode plates) for three days to allow the ion distribution to stabilize under gravity, as shown in the left panel of Figure 8. The stabilized voltage was then measured via a KEYSIGHT34465A meter. To avoid electromagnetic interference, the setup was enclosed in an iron cabinet during the measurements.

In previous experiments, the voltage was measured with no current flow. To determine whether a continuous current output could be sustained over time, a 6.8 M $\Omega$  resistor was connected across the electrodes of the vertically placed gravity cell. As shown in Figure 10, the left image illustrates the system in its stationary state, while the right image depicts the system with a 6.8 M $\Omega$  resistor connected between the positive and negative electrodes. The voltage was measured six times between the 15th and 55th days.

To test whether gravity truly caused the observed potential difference, the cells were inverted, allowing the solution to stabilize for 86 days. Voltage measurements were taken 24 times between the 33rd and 86th days, with the expectation that the inverted configuration would yield opposite voltage and current values.



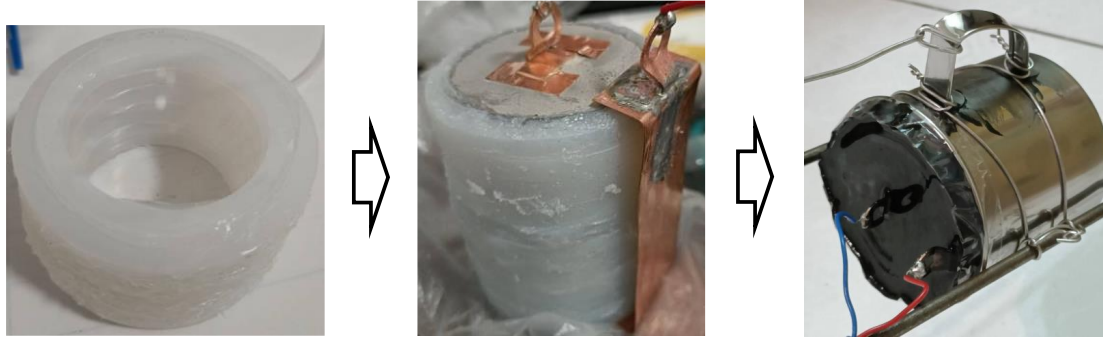


**Fig. 8.** Selected images of the gravity battery production process.

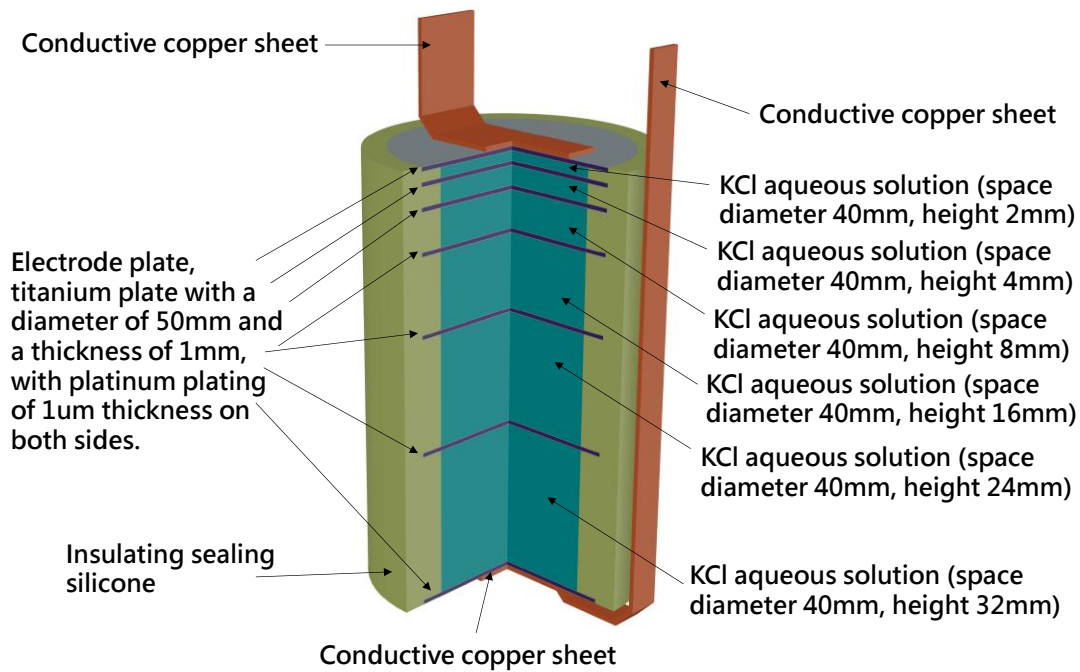


**Fig. 9.** Internal structure diagram of the gravity battery, including six small units with electrode spacings of 32 mm, 24 mm, 16 mm, 8 mm, 4 mm, and 2 mm that are electrically connected in series.



**Fig. 10.** Selected images of the gravity battery during the static measurement process.

### 2.2.2. *Experimental Results*

The left panel of Figure 11 shows the experimental setup, whereas the right panel illustrates the relationship between the output voltage and time under a 10 G centrifugal force field. As the 10G field was applied, the voltage difference between the two gravity batteries gradually increased, confirming that the centrifugal force induced potential changes in the solution along the direction of the field. This suggests that the device can continuously convert ambient thermal energy into electrical energy when exposed to a sufficiently large gravitational or centrifugal force. Small differences in pH between the two gravity batteries led to variations in the timing and magnitude of the generated potentials. Once the centrifuge stopped and no centrifugal force was applied, the

potential quickly returned to its initial state.

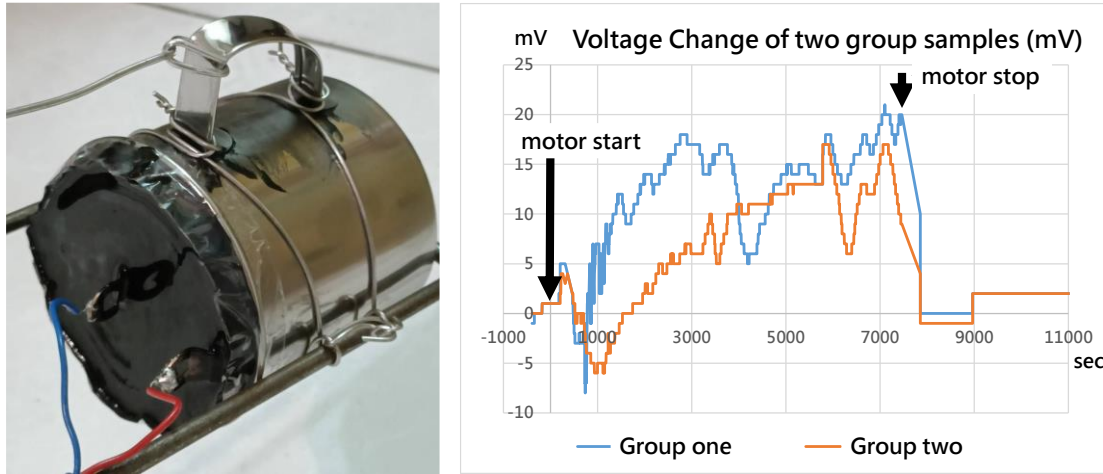


**Fig. 11.** The gravity battery unit was subjected to a centrifugal force field of 10 G (10 times the gravity of the Earth's surface), and the output voltage was continuously recorded for two hours. The resulting relationship between the measured potential and time is shown.

Table 2 summarizes the voltage measurements from the first and second samples when placed vertically with a 6.8 MΩ load from a resistor. The first sample exhibited an average output voltage of 22.594 mV with a standard deviation of 3.240 mV over 40 days (15<sup>th</sup> to 55<sup>th</sup>), whereas the second sample had an average output voltage of -0.647 mV with a standard deviation of 0.503 mV. Individual measurements for both samples are listed in the table.

Sample	Day 15	Day 25	Day 34	Day 41	Day 48	Day 55
1st	26.460 mV	25.571 mV	22.611 mV	19.423 mV	23.181 mV	23.181 mV
2nd	-0.331 mV	-0.123 mV	-0.272 mV	0.750 mV	-0.959 mV	-0.959 mV
Sample	Mean	Standard Deviation				
1st	22.594 mV	3.240 mV				
2nd	-0.647 mV	0.503 mV				

**Table 2.** Voltage measurements from the first and second samples when placed vertically with a 6.8 M $\Omega$  load from a resistor.

The data before the 15th day were discarded because the measurements taken before the 15th day were taken when the probe was in direct contact with the contacts of the gravity battery, so a small vibration would occur when the connection was made. This small vibration will cause turbulence in the electrolyte and destroy the stable state. After the 15th day, we switched to using fixed wires to connect to the electrodes of the gravity battery, and the probe was only in contact with the other end of the wire to eliminate the impact of vibration on the measurement. During the measurement process, we only used the first result, which was measured after the participants had stood for a whole night. When people move around the laboratory, the gas heated by a person's body temperature affects the ambient temperature, which flows through and contacts the gravity battery. This causes slight convection in the ionic aqueous solution in the gravity battery, causing it to deviate from the stable state.

To confirm that the potential difference is due to gravity, the opposite voltage should be measured when the gravity cell is turned upside down. When the same samples were placed upside down, the voltage began to change. The average output voltage of the first sample from the 33rd day to the 86th day was -4.169 mV, and the measurement standard deviation was 1.396 mV; the average output of the second sample was 11.148 mV, and the measurement standard deviation was 0.282 mV.

Table 3 summarizes the voltage measurements from the first and second samples when placed upside down with a 6.8 M $\Omega$  load from a resistor.

Sample	Day 33	Day 35	Day 37	Day 39	Day 41	Day 44
1st	-2.113 mV	-1.149 mV	-1.895 mV	-2.476 mV	-2.028 mV	-2.928 mV
2nd	11.702 mV	11.496 mV	11.241 mV	11.189 mV	10.871 mV	10.938 mV
Sample	Day 46	Day 48	Day 51	Day 53	Day 55	Day 58
1st	-5.729 mV	-6.162 mV	-5.669 mV	-4.141 mV	-3.860 mV	-4.732 mV
2nd	11.311 mV	10.733 mV	11.718 mV	11.302 mV	11.345 mV	11.244 mV
Sample	Day 60	Day 62	Day 65	Day 67	Day 69	Day 72
1st	-4.320 mV	-5.309 mV	-4.546 mV	-4.727 mV	-4.489 mV	-4.878 mV
2nd	11.362 mV	11.167 mV	10.909 mV	11.049 mV	11.215 mV	11.040 mV
Sample	Day 74	Day 76	Day 79	Day 81	Day 83	Day 86
1st	-4.066 mV	-4.959 mV	-4.295 mV	-6.263 mV	-5.091 mV	-4.234 mV
2nd	11.193 mV	11.204 mV	10.901 mV	11.064 mV	10.771 mV	10.577 mV
Sample	Mean	Standard Deviation				
1st	-4.169 mV	1.396 mV				
2nd	11.148 mV	0.282 mV				

**Table 3.** Voltage measurements from the first and second samples when placed upside down with a 6.8 M $\Omega$  load from a resistor.

The measurement results show that the output voltages of the upright and upside-down devices are opposite. Moreover, the voltage directions of the two samples are different when they are standing. According to our previous theoretical calculations, when the electrode exchanges electrons with different ions or when the pH is different, the voltage difference will be different and may be opposite.

In centrifugal force experiments, a voltage bias is generated because of the presence of a centrifugal force and disappears when the centrifugal force is removed, leading to the conclusion that the centrifugal force is responsible for the potential difference. In experiments directly utilizing Earth's gravity, stable current and electrical energy output were maintained regardless of whether the system was placed upright or inverted, indicating that this voltage difference is not

limited to a temporary state but represents a stable, steady condition. These experiments demonstrate that continuous energy conversion occurs in both gravitational and centrifugal force fields. According to the law of conservation of energy and supported by earlier theoretical derivations, the energy source is identified as the thermal energy from the environment. Our measurements are consistent with the phenomenon observed by T. Dale Stewart and Richard C. Tolman in 1910.<sup>4</sup>

### **3. DISCUSSION**

When a force acts on the same physical properties of ions, since the ions move in a random and scattered manner, it must comply with Carnot's theorem,<sup>1</sup> which states that the maximum energy output rate of a heat engine cannot be greater than the temperature difference divided by the absolute temperature. However, when an electric field affects the charge of an ion, gravity affects the mass of the ion. The forces experienced by ions with different masses are unequal, imparting directional characteristics to ion motion. This article raises the question of whether, in cases where ions of different masses exhibit diverse directional tendencies, it might be possible to surpass the constraints imposed by Carnot's theorem.<sup>1</sup> In our theoretical derivation, a potential difference caused by gravity is indeed derived. Therefore, it is possible to convert thermal energy into electrical energy without a temperature difference.

Although the initial theoretical derivations were based on plasma, practical experiments with ion plasma are challenging because ion plasma extraction is difficult to perform via centrifugation; therefore, we opted instead to conduct experiments using aqueous ion solutions with ions of different masses or mass-charge ratios. The first aqueous ion solution to be considered is sodium chloride, which is the easiest to obtain. Chloride ions and sodium ions have the same charge and

opposite electrical properties, and the ion masses greatly differ, so they may be good experimental objects. However, when the buoyancy force on the effective volume in solution is considered, because the volume of chloride ions is much larger than that of sodium ions, after the buoyancy force is deducted, the net masses of the two ions will be very close, so observing the voltage difference due to gravity is difficult. Therefore, we changed the solution to a potassium chloride aqueous solution with similar original masses of positive and negative ions but a large difference in effective volume. As we calculated in the previous article, there is a large difference in the net masses of chloride ions and potassium ions. In the experiment, the potential difference was indeed measured when the sample was placed upright and upside down. That is, the same sample will have different potential differences in different directions of gravity. It can also be inferred that the voltage difference is caused by gravity.

In limited measurements, the voltage and current that can be measured are very small, but it can still be proven that thermal energy is converted into electrical energy without a temperature difference.

To amplify the energy output, either increasing the rotational speed or reducing the radius can be effective strategies. A faster rotating centrifuge can significantly increase the energy output. As mentioned in the article, for the same rotation radius and the same amount of electrolyte, when the rotational speed is doubled, appropriate structural modifications can produce sixteen times the output, whereas the energy lost to air resistance increases by only approximately four times. Therefore, increasing the rotational speed must increase the electrical energy output more than the energy lost to air resistance.

Similarly, reducing the rotation radius also contributes to a higher energy output. Since air resistance is proportional to the square of the rotational speed, a smaller radius allows the

same acceleration to be achieved at a slower rotational speed, which corresponds to lower air resistance. Additionally, for the same rotational speed, a smaller radius results in a greater centrifugal force. This means that reducing the radius can achieve comparable acceleration with lower frictional losses, providing an efficient way to increase the energy output.

In terms of energy conversion efficiency. Potassium chloride is not the most energy-efficient combination of ingredients, but many other chemical combinations could be tested.

#### **4. CONCLUSION**

Energy conversion is crucial for the sustainable operation of our planet. While concentration cells have been extensively studied and applied, the potential difference caused by concentration gradients resulting from gravity or centrifugal force has not received sufficient attention. With the insight provided by Richard C. Tolman's 1910 observation of voltage bias in conductors within an accelerated force field, it becomes clear that such forces can indeed generate a potential difference<sup>4</sup>. Our theoretical calculations confirm that this potential difference occurs not only on the surface of the conductor but also within its interior, further suggesting that thermal energy can be converted into electrical energy even in the absence of a temperature difference. We demonstrated this experimentally by using a centrifugal force or artificial gravity to generate a potential difference. Furthermore, by utilizing natural gravity, we achieve a continuous current output. The reversal of the output voltage when the device is inverted further verifies that gravity can indeed produce a voltage difference and current.

This study concludes that, in the absence of a temperature gradient, the use of gravity or a centrifugal force provides a feasible method for converting thermal energy into electrical energy, thereby overcoming the limitations imposed by Carnot's theorem. Although the mechanism for



counteracting changes in ion concentration still requires further study, this approach holds promise as a viable green energy source. This discovery opens new avenues for research and practical applications in various directions.

## **ACKNOWLEDGMENTS**

We would like to acknowledge the professional manuscript services of American Journal Experts. Additionally, we extend our sincere gratitude to Wolfgang Sturm for providing valuable insights into the 'Stewart–Tolman effect', which greatly facilitated access to prior experimental results.

## **DATA AVAILABILITY STATEMENT**

Not applicable

## **DECLARATIONS**

### **Conflict of interest statement**

The author has no conflicts of interest to disclose.

### **Author Contributions**

Kuo Tso Chen designed the study, performed the experiments, analyzed the data, and wrote the manuscript.

## **Ethics Approval**

I confirm that the manuscript has been approved by the author for publication. I declare that the work described herein is original research and that it has not been published previously.

## REFERENCES

- <sup>1</sup>Y. Izumida, "Irreversible efficiency and Carnot theorem for heat engines operating with multiple heat baths in linear response regime," *Phys. Rev. Res.* 4, 023217 (2022).
- <sup>2</sup>M. R. Morad, F. Momeni, "On the proof of the first Carnot theorem in thermodynamics," *Eur. J. Phys.* 34, 1581–1588 (2013).
- <sup>3</sup>Milivoje M. Kostic, "The Second Law and Entropy Misconceptions Demystified", *Entropy* 2020, 22(6), 648 (2020), <https://www.mdpi.com/1099-4300/22/6/648> , Accessed 13 November 2024.
- <sup>4</sup>R.C. Tolman, "The Electromotive Force Produced in Solutions by Centrifugal Action", *Proc. Am. Acad. Arts Sci.* 46, 109 (1910),
- <sup>5</sup>R. C. Tolman, and T. D. Stewart, "The electromotive force produced by the acceleration of metals," *Phys. Rev.* 8, 97–116 (1916).
- <sup>6</sup>Colley, R., "Nachweis der Existenz der Maxwellschen electromotorischen Kraft". *Wiedemann's Annalen der Physik*, 17, 55-70.(1882)
- <sup>7</sup>Des Coudres, Th., "Nachweis der Existenz der Maxwellschen electromotorischen Kraft". *Annalen der Physik*, 49, 284-300.(1893).
- <sup>8</sup>L. Lao, C. Ramshaw, H. Yeung, "Process intensification: water electrolysis in a centrifugal acceleration field", *Journal of Applied Electrochemistry*, 41, 645-656, (2011). <https://link.springer.com/article/10.1007/s10800-011-0275-2>.
- <sup>9</sup>Bennett, Charles H. "The thermodynamics of computation—a review.", *International Journal of Theoretical Physics* 21.12 (1982): 905-940.
- <sup>10</sup>J. W. Gibbs, *Elementary Principles in Statistical Mechanics* (Charles Scribner's Sons, 1902).
- <sup>11</sup>P. J. Mohr, D. B. Newell, and B. N. Taylor, "2014 CODATA recommended values of the fundamental constants of physics and chemistry," (2014), Accessed 8 June 2023, [https://physics.nist.gov/cuu/pdf/wallet\\_2014.pdf](https://physics.nist.gov/cuu/pdf/wallet_2014.pdf).
- <sup>12</sup>T. Prohaska, J. Irrgeher, J. Benefield, J. K. Böhlke, L. A. Chesson, T. B. Coplen, T. Ding, P. J. H. Dunn, M. Gröning, N. E. Holden, H. A. J. Meijer, H. Moossen, A. Possolo, Y. Takahashi, J. Vogl, T. Walczyk, J. Wang, M. E. Wieser, S. Yoneda, X.-K. Zhu, and J. Meija, "Standard atomic weights of the elements 2021 (IUPAC Technical Report)," *Pure Appl. Chem.* 94, 573–600 (2022).
- <sup>13</sup>P. J. Mohr, D. B. Newell, and B. N. Taylor, *CODATA Recommended Values of the Fundamental Physical Constants: 2014* (National Institute of Standards and Technology, 2015).
- <sup>14</sup>Rosemount, "CONDUCTANCE DATA FOR COMMONLY USED CHEMICALS", EMERSON Process Management, 44-6039/rev. B, December 2010, Accessed 2023/06/15 [https://www.emerson.com/documents/automation/manual-conductance-data-for-commonly-used-chemicals-en-68896.pdf?fbclid=IwZXh0bgNhZW0CMTAAAR28aYEXbKjQYIFozzqztvH7KBwrGrKL5xI3K2oxpY21IeCrGCSa0hR6dM\\_aem\\_M2k4ygz8ZCJzwnsialdOJA](https://www.emerson.com/documents/automation/manual-conductance-data-for-commonly-used-chemicals-en-68896.pdf?fbclid=IwZXh0bgNhZW0CMTAAAR28aYEXbKjQYIFozzqztvH7KBwrGrKL5xI3K2oxpY21IeCrGCSa0hR6dM_aem_M2k4ygz8ZCJzwnsialdOJA).
- <sup>15</sup>D. Rowland, "Density of hydrochloric acid, HCl(aq), advanced thermodynamics," *Advanced Thermodynamics*, 2021, Accessed 8 June 2023, [https://advancedthermo.com/electrolytes/density\\_HCl.html](https://advancedthermo.com/electrolytes/density_HCl.html).
- <sup>16</sup>D. Rowland, "Density of potassium chloride, KCl(aq), advanced thermodynamics," *Advanced Thermodynamics*, 2021, Accessed 8 June 2023, [https://advancedthermo.com/electrolytes/density\\_KCl.html](https://advancedthermo.com/electrolytes/density_KCl.html).

<sup>17</sup>D. Larsen, "20.6: The Nernst equation1. Chemistry libretexts," (2016), Accessed 7 November 2023,  
[https://chem.libretexts.org/Courses/Heartland\\_Community\\_College/HCC%3A\\_Chem\\_162/20%3A\\_Electrochemistry/20.6%3A\\_The\\_Nernst\\_Equation](https://chem.libretexts.org/Courses/Heartland_Community_College/HCC%3A_Chem_162/20%3A_Electrochemistry/20.6%3A_The_Nernst_Equation).